SUPPLEMENTARY INFORMATION FOR

Using population dynamics to count bacteriophages and their lysogens

Yuncong Geng[1,2,#], Thu Vu Phuc Nguyen[1,3,4,#], Ehsan Homaee[1,2], Ido Golding[1,2,3,5*]

[1]Department of Physics, University of Illinois Urbana-Champaign, Urbana, IL 61801, USA
[2]Center for Biophysics and Quantitative Biology, University of Illinois Urbana-Champaign, Urbana, IL 61801, USA
[3]Verna and Marrs McLean Department of Biochemistry and Molecular Biology, Baylor College of Medicine, Houston, TX 77030, USA
[4]Present address: Department of Molecular Biology, Princeton University, Princeton, NJ 08544, USA
[5]Department of Microbiology, University of Illinois Urbana-Champaign, Urbana, IL 61801, USA
[#]*Y.G. and T.V.P.N. contributed equally to this work*
**Corresponding author (igolding@illinois.edu)*

This file includes:

SUPPLEMENTARY FIGURES

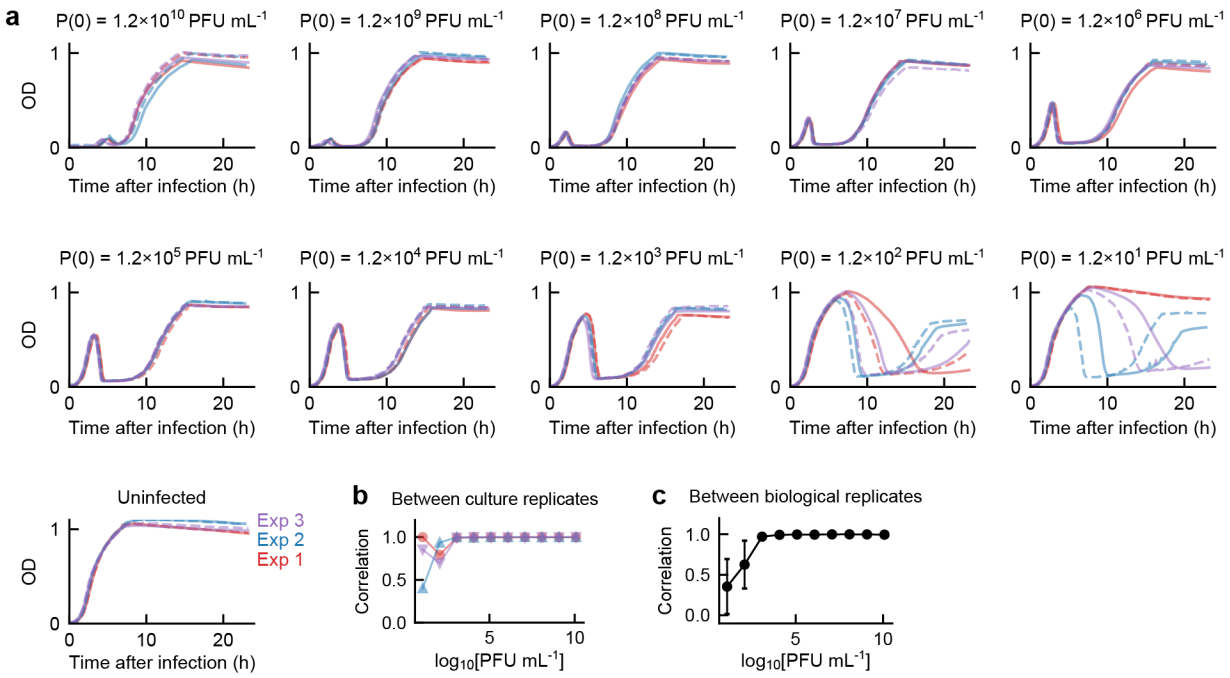

Supplementary Fig. 1: Reproducibility of the bacterial growth curves and the OD-based phage counting method.

(**a**) Representative growth curves of *E. coli* MG1655 cultures at 37ºC in LBM infected by λ_{ts} at different concentrations (three experiments, different colors). For each initial phage concentration ($P(0)$) and each experiment, growth curves of two culture replicates (solid and dashed lines) are shown. The experimental protocol is described in **Methods**, "Microplate-based infection assay for measuring phage concentrations". (**b**) The reproducibility of growth curves among culture replicates. Markers, Pearson correlation coefficients of the growth curves from $n = 2$ culture replicates infected at a given initial phage concentration in each of the three experiments (as in panel a). (**c**) The reproducibility of growth curves among biological replicates. Markers, Pearson correlation coefficients of the growth curves infected at a given initial phage concentration (as in panel a), calculated with bootstrapping ($N = 1000$) from all culture replicates across the three biological replicates. Error bar, standard error of the mean (SEM).

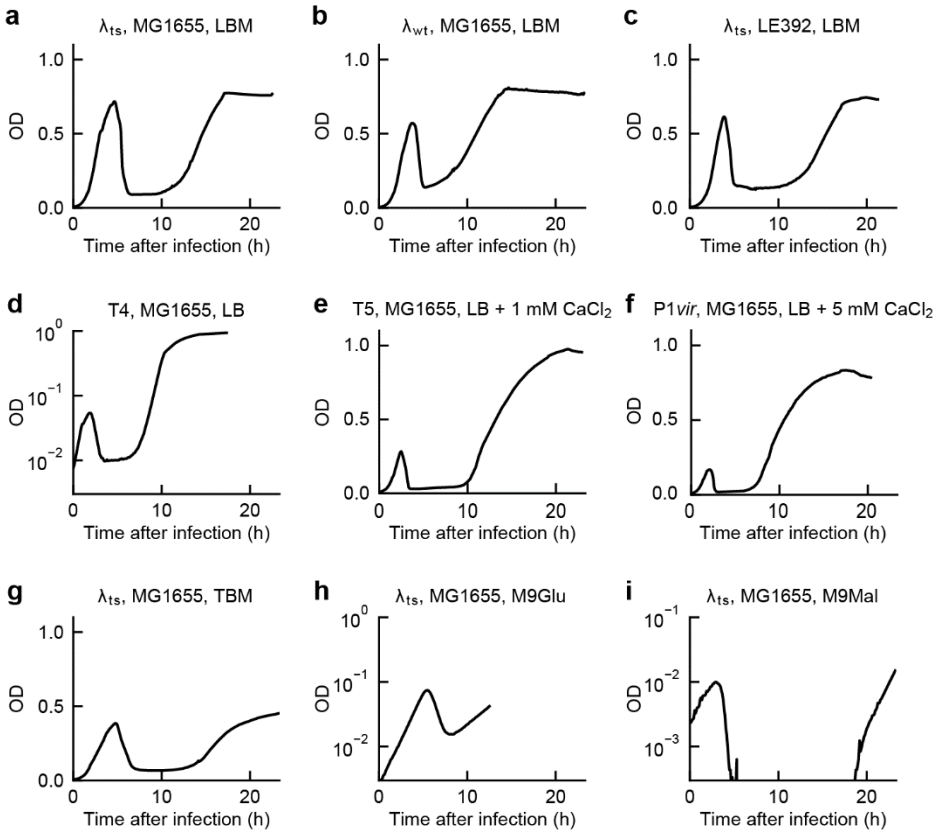

Supplementary Fig. 2: Representative growth curves of bacterial cultures infected by different phages and in different growth media.

(**a-i**) Lines, growth curves of MG1655 cultures infected at 37ºC. The initial phage concentration for each infection condition ranges between ≈ 1×10^4 PFU mL^{-1} and ≈ 7×10^4 PFU mL^{-1}. For infection by phage T4 (panel d) and infections in minimal media (panels h and i), the y-axes are displayed on a logarithmic scale.

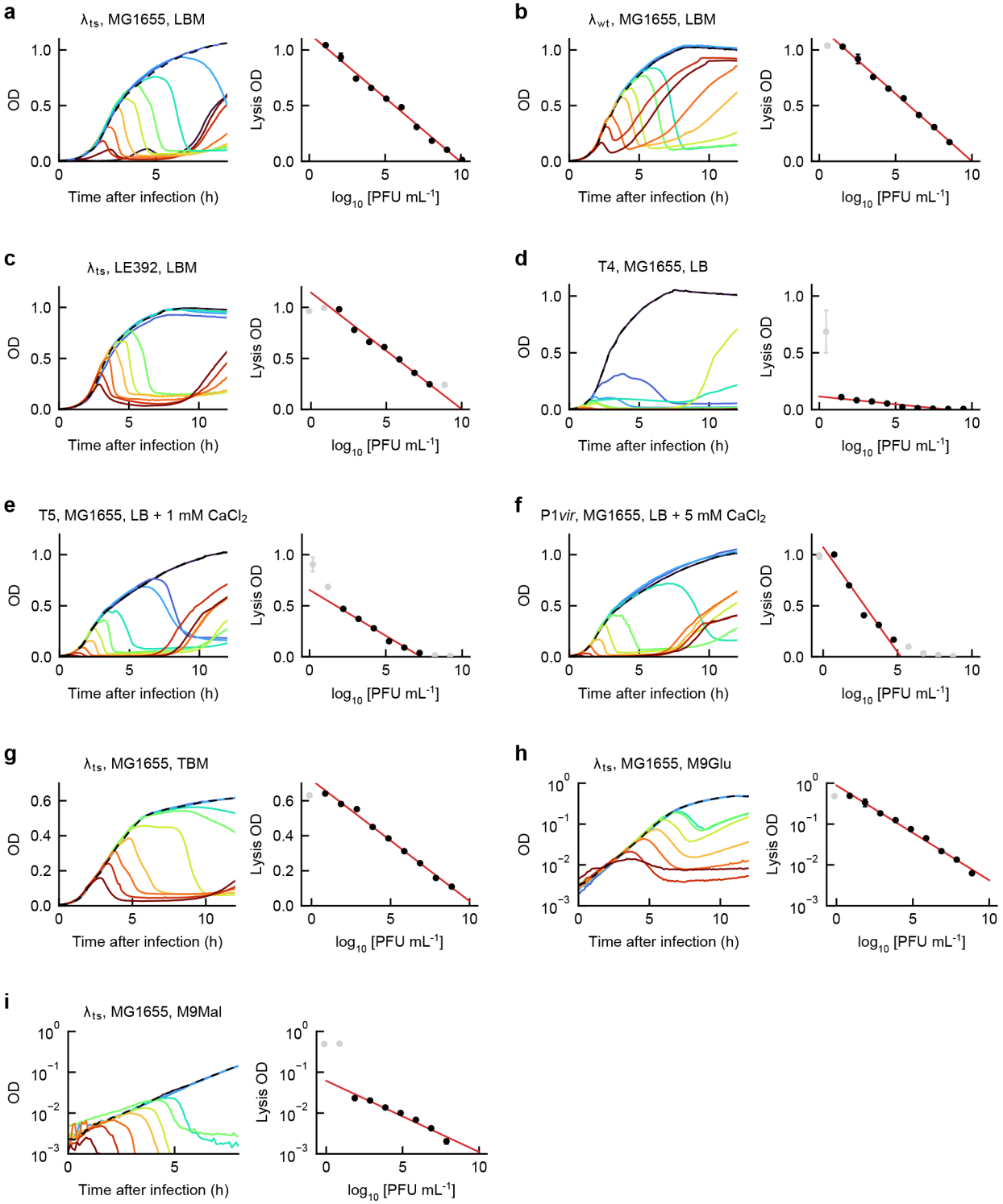
a
λts, MG1655, LBM
b
λwt, MG1655, LBM
c
λts, LE392, LBM
d
T4, MG1655, LB
e
T5, MG1655, LB + 1 mM CaCl2
f
P1vir, MG1655, LB + 5 mM CaCl2
g
λts, MG1655, TBM
h
λts, MG1655, M9Glu
i
λts, MG1655, M9Mal
OD
Lysis OD
Time after infection (h)
log10 [PFU mL-1]

Supplementary Fig. 3: Calibration curves for counting phages under different infection conditions.

The infection conditions in this figure correspond to those in **Supplementary Fig. 2**. In each panel, left, solid lines, growth curves of *E. coli* cultures infected at different phage concentrations (red to blue, high to low phage concentrations). Dashed line, growth curve of an uninfected culture. Right, black markers, data used to fit the calibration curve. Error bars, SEM from culture replicates (n = 2 or n = 4). Gray markers, data not used for fitting. Red line, linear fit ($y = k \cdot x + b$). For infections in minimal media (panels h and i), the y-axes are displayed on a logarithmic scale. The fitting procedure is described in **Methods**, "Microplate-based infection assay for measuring phage concentrations". The range of phage concentrations and the fitted parameter values for each infection condition are as follows.

(**a**) From ≈ 1.2×10^{1} PFU mL^{-1} to ≈ 1.2×10^{10} PFU mL^{-1}, with $k = -0.115 \pm 0.002$, $b = 1.15 \pm 0.02$.
(**b**) From ≈ 3.4×10^{0} PFU mL^{-1} to ≈ 3.4×10^{8} PFU mL^{-1}, with $k = -0.121 \pm 0.004$, $b = 1.21 \pm 0.03$.
(**c**) From ≈ 7.4×10^{-1} PFU mL^{-1} to ≈ 7.4×10^{8} PFU mL^{-1}, with $k = -0.114 \pm 0.005$, $b = 1.15 \pm 0.03$.
(**d**) From ≈ 2.8×10^{0} PFU mL^{-1} to ≈ 2.8×10^{9} PFU mL^{-1}, with $k = -0.014 \pm 0.001$, $b = 0.12 \pm 0.01$.
(**e**) From ≈ 1.6×10^{0} PFU mL^{-1} to ≈ 1.6×10^{9} PFU mL^{-1}, with $k = -0.090 \pm 0.005$, $b = 0.66 \pm 0.02$.
(**f**) From ≈ 5.5×10^{-1} PFU mL^{-1} to ≈ 5.5×10^{8} PFU mL^{-1}, with $k = -0.21 \pm 0.02$, $b = 1.07 \pm 0.06$.
(**g**) From ≈ 7.4×10^{-1} PFU mL^{-1} to ≈ 7.4×10^{8} PFU mL^{-1}, with $k = -0.069 \pm 0.002$, $b = 0.72 \pm 0.01$.
(**h**) From ≈ 7.4×10^{-1} PFU mL^{-1} to ≈ 7.4×10^{8} PFU mL^{-1}, with $k = -0.23 \pm 0.01$, $b = -0.05 \pm 0.06$.
(**i**) From ≈ 7.4×10^{-1} PFU mL^{-1} to ≈ 7.4×10^{8} PFU mL^{-1}, with $k = -0.17 \pm 0.01$, $b = -1.21 \pm 0.07$.

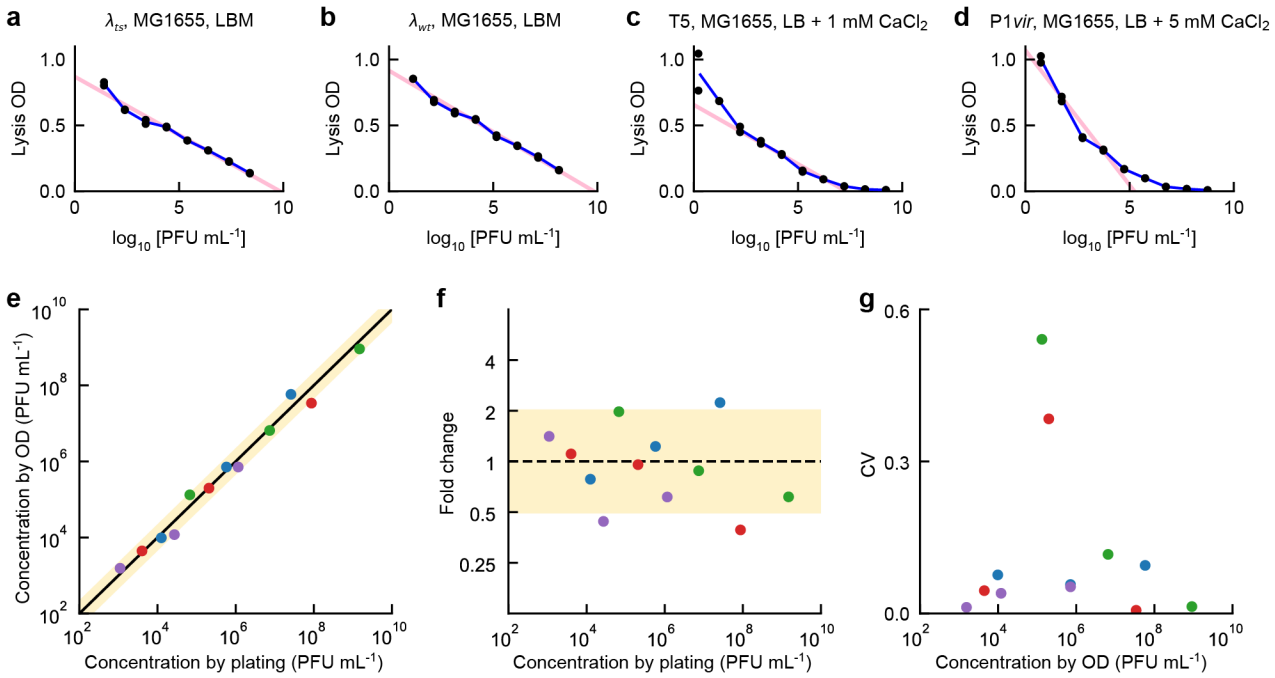

Supplementary Fig. 4: Accuracy and precision of OD-based counting when interpolating between adjacent calibration points.

(**a-d**) Calibration curves for (**a**) λ_{ts}, (**b**) λ_{wt}, (**c**) T5, and (**d**) P1*vir*. Markers, data. Pink lines, linear calibration curves (used in calculating the data shown in **Figs. 2c-e**). Blue lines, interpolation between adjacent calibration points (used in calculating the data shown in panels e-g below). (**e**) Comparison of phage concentrations measured using the OD-based method and traditional plaque assay. Samples of λ_{ts}, λ_{wt}, T5, and P1*vir* (green, red, blue, and purple, respectively), each phage at three different concentrations, were enumerated using the two methods. Markers, mean; error bars, SEM from $n = 2$ culture replicates. Black line, $y = x$. Yellow shading, fold change ≤ 2 from the black line. (**f**) The accuracy of OD-based phage counting. The fold change between the phage concentrations measured using the OD-based method and the plaque assay, calculated using the data in panel b, is plotted. Markers, mean; error bars, SEM from $n = 2$ culture replicates. Yellow shading, fold change ≤ 2. (**g**) The precision of OD-based phage counting. The coefficient of variation (CV) between the culture replicates ($n = 2$) for a given sample is plotted.

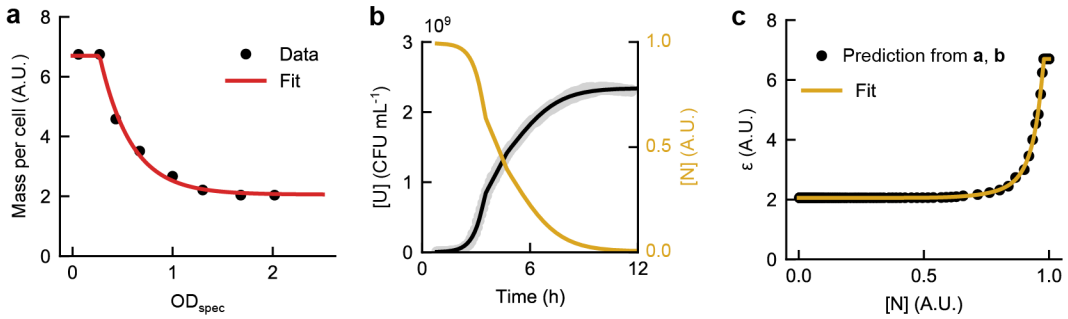

Supplementary Fig. 5: Parameterization of the cell density-to-OD conversion.

(**a**) Mass per cell as a function of OD_{spec}, adapted from Sezonov *et al.*[1], where mass per cell is defined as the ratio of OD_{spec} to the cell concentration, multiplied by 10^9. (**b**) A model describing nutrient-dependent growth (black) captures the cell density dynamics of uninfected cultures (gray); gold, the inferred time-dependent nutrient abundance. (**c**) A polynomial fit (gold) captures the relative absorptivity as a function of nutrient concentration (black). The data analysis procedure is described in **Methods**, "Parameterization of cell growth".

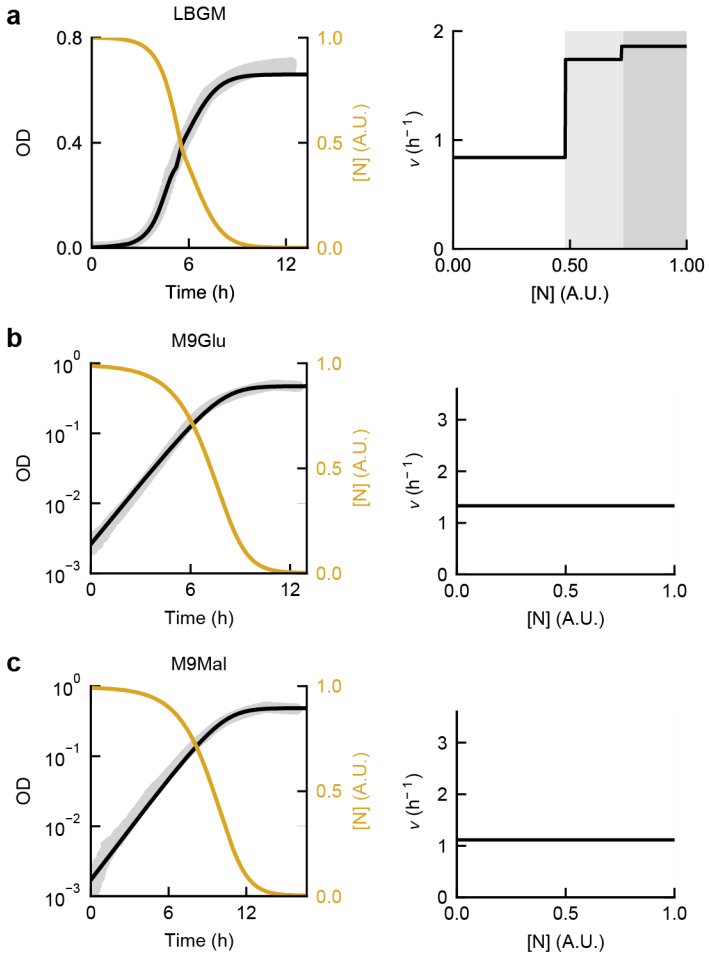

Supplementary Fig. 6: Parameterization of bacterial growth.

(**a-c**) MG1655 cells were grown in different growth media at 37ºC. In each panel, left, a model describing nutrient-dependent growth (black) captures the measured OD dynamics of uninfected cultures (gray); gold, the inferred time-dependent nutrient abundance. Right, the maximum growth rate v (black) at different stages of nutrient consumption (white and gray shading). The fitted parameters are shown in **Supplementary Table 2**. The modeling for cell growth is described in **Methods**, "Parameterization of cell growth".

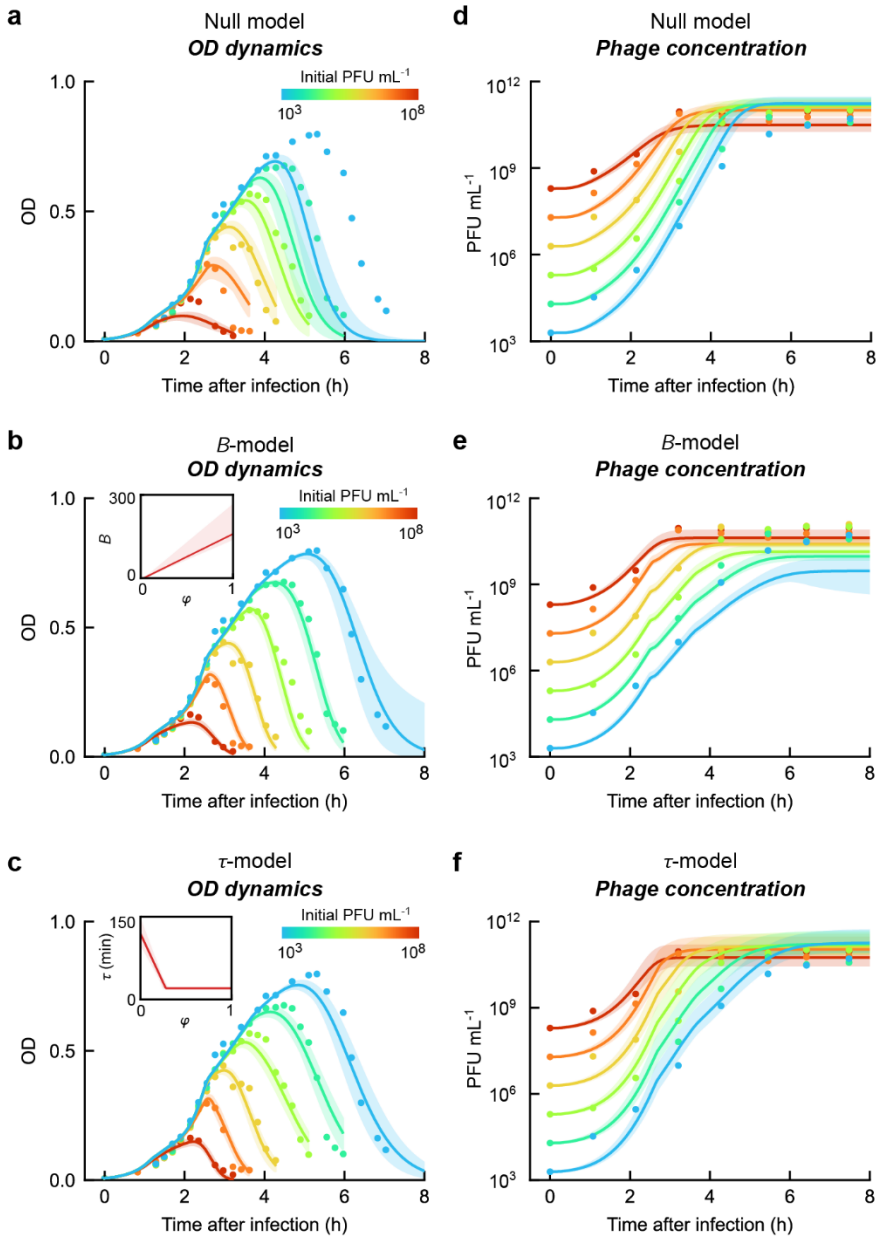
a
Null model
OD dynamics
Initial PFU mL-1
10^3
10^8
OD
Time after infection (h)
d
Null model
Phage concentration
PFU mL-1
Time after infection (h)
b
B-model
OD dynamics
B
φ
e
B-model
Phage concentration
c
τ-model
OD dynamics
τ (min)
f
τ-model
Phage concentration

Supplementary Fig. 7: Modeling infection dynamics under different growth-rate dependencies.

(**a-c**) Model fitting for the OD dynamics. The models tested are (**a**) "null model": r, B, and τ are constant, (**b**) "B-model": r and τ are constant, and $B = \max(0, B_k \cdot \varphi + B_0)$, and (**c**) "$\tau$-model": r and B are constant, and $\tau = \max(20, \tau_k \cdot \varphi + \tau_0)$. In each panel, colored markers, data from infection at different initial phage concentrations. Colored lines, best fit of the model. Colored shading, fits by the ensemble of parameters obtained using Markov chain Monte Carlo (MCMC). Inset, fitted infection parameter as a function of normalized instantaneous growth rate φ. (**d-f**) Prediction of the phage dynamics, by the (**d**) "null model", (**e**) "B-model" and (**f**) "τ-model". In each panel, colored markers, data from infection at different initial phage concentrations. Colored lines, model predictions from the best-fit parameters. Colored shading, model predictions from the ensemble of parameters. The corresponding results for the "r-model" are shown in **Figs. 3c** and **3e**. The fitting and prediction procedures are described in **Methods**, "Parameterization of phage-cell encounter rate, latent period, and burst size", "Characterizing the dependence of infection parameters on growth rate", and "Predicting phage dynamics for infection in LBM". The fitted parameters are shown in **Supplementary Table 3**.

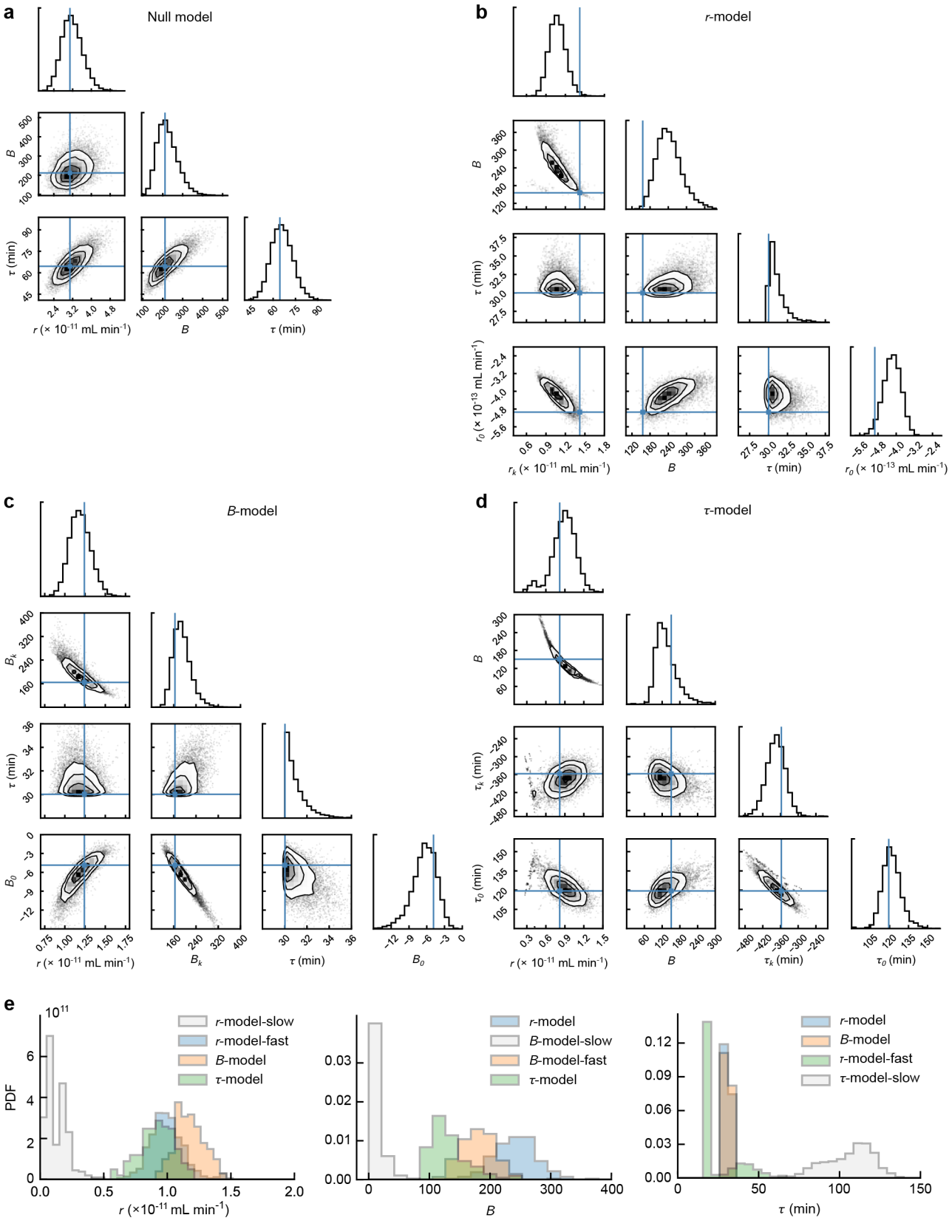
a
Null model
b
r-model
c
B-model
d
τ-model
e
r-model-slow
r-model-fast
B-model
τ-model
PDF
r (× 10^-11 mL min^-1)
B
τ (min)
r-model
B-model-slow
B-model-fast
τ-model
r-model
B-model
τ-model-fast
τ-model-slow

Supplementary Fig. 8: Comparison of inferred parameters under different growth-rate dependencies.

(**a-d**) The distribution of phage-cell encounter rate r, burst size B, and latent period τ, and their dependencies on the normalized instantaneous growth rate (φ). The models shown are (**a**) "null model", (**b**) "r-model", (**c**) "B-model" and (**d**) "τ-model". In each panel, the marginal distribution of the parameters is shown on the diagonal, and the joint distribution of pairs of parameters is shown off-diagonal. Blue line indicates the best-fit parameter value. **(e)** Comparison of the distribution of r (left), B (middle), and τ (right) from the different models ("r-model", "B-model" and "τ-model"). For models in which the parameter is growth rate-independent, the posterior distribution from MCMC is shown. For models in which the parameter is growth rate-dependent, we integrate the posterior distribution with the growth rate distribution throughout the infection processes; the resulting distribution is divided into a population representing the parameters at fast-growing conditions (doubling time $\lesssim 30$ min) and another population representing the parameters at slow-growing conditions (doubling time > 30 min, in gray). The fitting procedure is described in **Methods**, "Parameterization of phage-cell encounter rate, latent period, and burst size" and "Characterizing the dependence of infection parameters on growth rate",. The fitted parameters are shown in **Supplementary Table 3**.

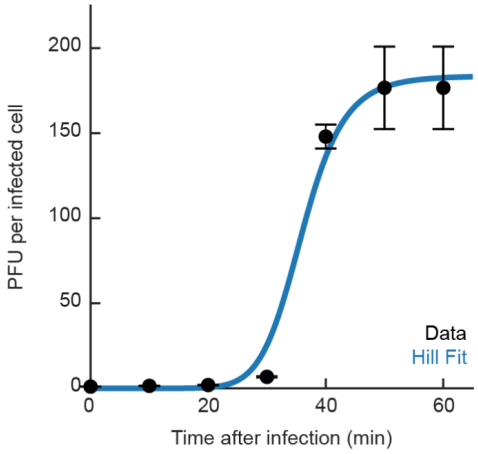

Supplementary Fig. 9: One-step growth curve for infection of MG1655 by λ_{ts}.

Infection was performed as described in ref. [2]. Briefly, cells were cultured in LBMM at 37°C, infected at MOI ≈ 0.1, diluted into pre-warmed LBGM, and grown at 37°C with aeration. At each sampled time point, infected cells were aliquoted and immediately assayed for the phage concentration using the plaque formation assay. The numbers of PFU per infected cell were calculated by normalizing the measured phage concentrations by the value at 0 minutes. Markers, data; error bars, SEM between plating replicates. Blue curve, Hill fit ($y = (ax^n)/(k^n + x^n)$). Burst size (estimated using the parameter a), 184 ± 28 PFU per cell. Latent period (estimated using the parameter k), 36.0 ± 3.3 min. For comparison with model-inferred values, see **Supplementary Table 3**.

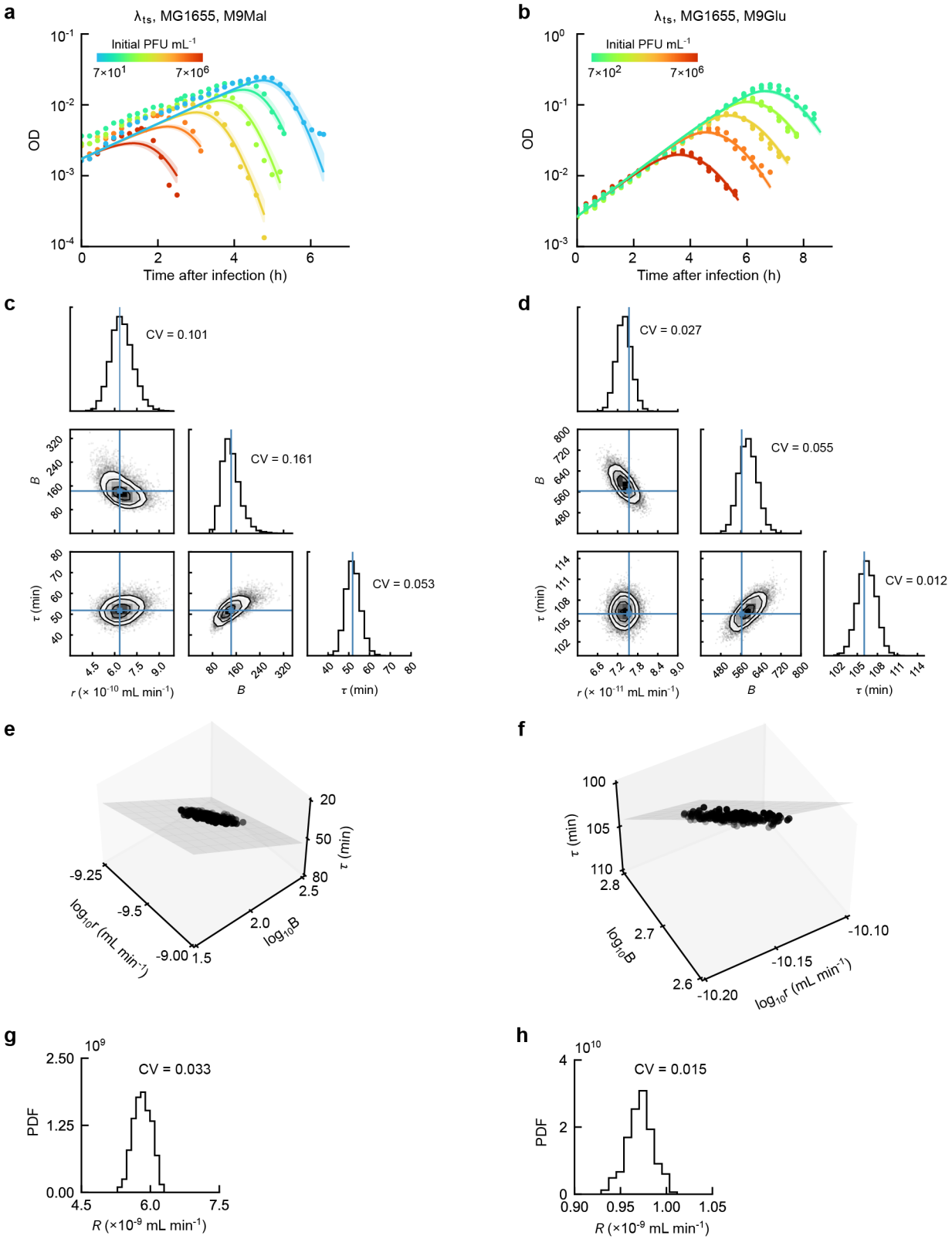
a
λts, MG1655, M9Mal
Initial PFU mL-1
7×10^1
7×10^6
OD
Time after infection (h)
b
λts, MG1655, M9Glu
Initial PFU mL-1
7×10^2
7×10^6
OD
Time after infection (h)
c
CV = 0.101
CV = 0.161
CV = 0.053
B
τ (min)
r (× 10^-10 mL min^-1)
B
τ (min)
d
CV = 0.027
CV = 0.055
CV = 0.012
B
τ (min)
r (× 10^-11 mL min^-1)
B
τ (min)
e
log10r (mL min^-1)
log10B
τ (min)
f
τ (min)
log10B
log10r (mL min^-1)
g
CV = 0.033
PDF
R (×10^-9 mL min^-1)
h
CV = 0.015
PDF
R (×10^-9 mL min^-1)

Supplementary Fig. 10: Modeling infection dynamics in minimal media.

(**a-b**) Fitted OD dynamics for infection in (**a**) M9Mal and (**b**) M9Glu. In each panel, colored markers, data from infection at different initial phage concentrations. Colored lines, best fit of the model. Colored shading, fits by the ensemble of parameters obtained using Markov chain Monte Carlo (MCMC). (**c-d**) The distribution of phage-cell encounter rate r, burst size B, and latent period τ for infection in (**c**) M9Mal and (**d**) M9Glu. In each panel, the marginal distribution of the parameters is shown on the diagonal, and the joint distribution of pairs of parameters is shown off-diagonal. Blue line indicates the best-fit parameter value. The fitting procedure is described in **Methods**, "Characterizing the relative growth rate of the viral population". The fitted parameters are shown in **Supplementary Table 3**. (**e-f**) Scatter plot of $\log_{10} r$, $\log_{10} B$ and τ in 3D, for infection in (**e**) M9Mal and (**f**) M9Glu. Markers, the ensemble of parameters obtained using MCMC. Grey shading, fitted plane: $\tau = \alpha * [\log_{10} r + \log_{10} B] + \beta$, where $g^* = \ln 10 / \alpha$. For (**e**) M9Mal, α = 44.1 $\pm$ 0.7, β = -34.1 $\pm$ 1.3, g^* = 0.052 $\pm$ 0.001 min^{-1}. For (**f**) M9Glu, α = 65.0 $\pm$ 1.7, β = 0.02 $\pm$ 2.79, g^* = 0.035 $\pm$ 0.001 min^{-1}. (**g-h**) The distribution of R for infection in (**g**) M9Mal and (**h**) M9Glu.

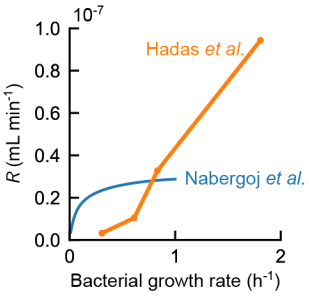

Supplementary Fig. 11: The relative growth rate of phage T4.

The relative growth rate of the viral population (R) for phage T4 as a function of bacterial growth rate, calculated from the data reported in Nabergoj *et al.*[3] (blue) and Hadas *et al.*[4] (orange). The data analysis procedure is described in **Methods**, "Characterizing the relative growth rate of the viral population".

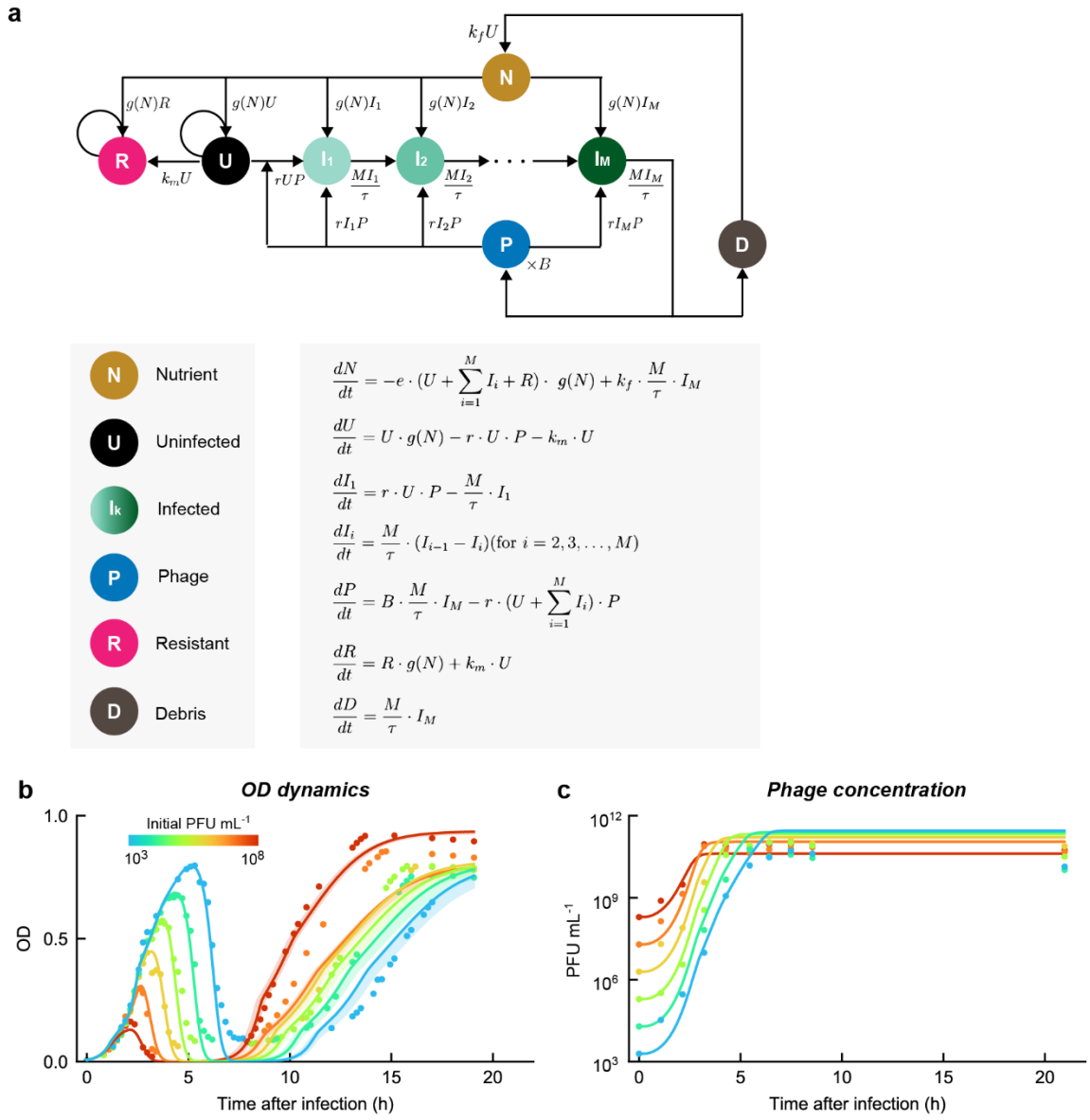

Supplementary Fig. 12: Modeling bacterial recovery following phage infection.

(**a**) A model with a transition from phage-sensitive to resistant cells. Circles, species tracked by the model. Arrows, transitions between species. The transition rates are indicated next to the corresponding arrows. (**b**) Model fitting for the OD dynamics. Colored markers, data from infection at different initial phage concentrations. Colored lines, best fit of the model. Colored shading, fits by the ensemble of parameters obtained using Markov chain Monte Carlo (MCMC). (**c**) Prediction of the phage dynamics. Colored markers, data from infection at different initial phage concentrations. Colored lines, model predictions from the best-fit parameters. Colored shading, model predictions from the ensemble of parameters. The fitted parameters are as follows: $k_m = (5.5 \pm 0.8) \times 10^{-8}$ min^{-1}, $k_f = 0.379 \pm 0.004$, where the errors represent the standard deviation over the ensemble of parameters. The fitting and prediction procedures are described in **Methods**, " Modeling bacterial recovery". Parameters related to cell growth are shown in **Supplementary Table 2**. The remaining parameters (r, B and τ) are shown in **Supplementary Table 3**.

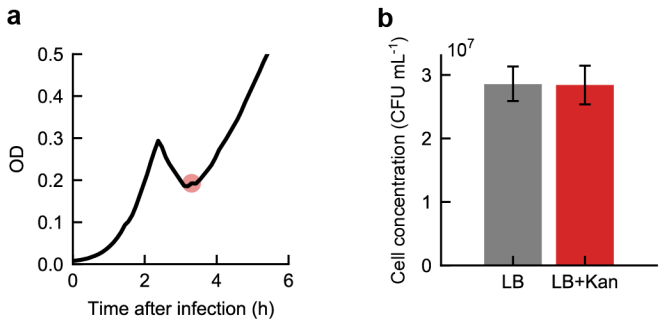

Supplementary Fig. 13: Quantifying the proportion of lysogens among surviving cells in phage-infected cultures.

MG1655 cells were infected by temperate phage λ_{wt}, as described in **Methods**, "Quantifying the proportion of lysogens among surviving cells in phage-infected cultures". (**a**) The growth curve following infection at an initial phage concentration of $\approx 2 \times 10^7$ PFU mL^{-1}. Red circle, the point at which the culture was extracted for colony plating. (**b**) Gray bar, total cell concentration ($(2.85 \pm 0.26) \times 10^7$ CFU mL^{-1}), obtained by plating on non-selective LB agar plates. Red bar, concentration of lysogenic cells ($(2.84 \pm 0.31) \times 10^7$ CFU mL^{-1}), obtained by plating on LB agar plates supplemented with 50 μg mL^{-1} kanamycin. Error bars, SEM from dilution and plating replicates.

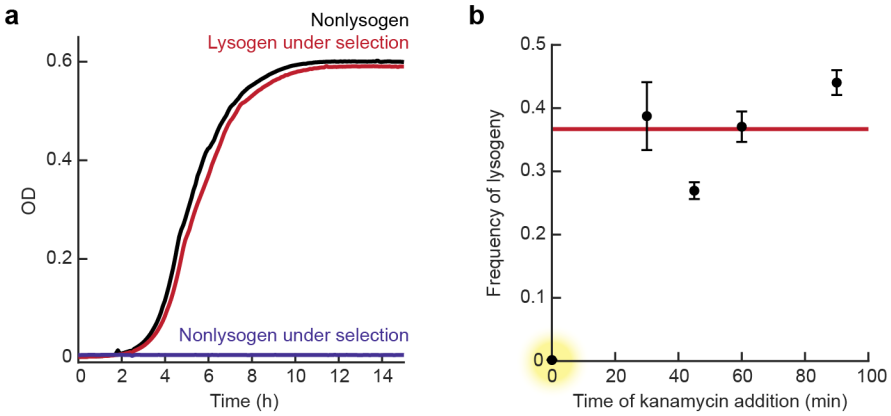

Supplementary Fig. 14: Using kanamycin to select for lysogenic cells.

(**a**) The growth curves of MG1655 without kanamycin selection (black) and under selection of 50 μg mL^{-1} kanamycin (violet), and of lysogenic cells (MG1655 λ_{ts}) under selection (red). All cultures were inoculated using similar concentrations of cells, and grown in LBGM at 30°C. (**b**) The frequency of lysogeny (measured as described in **Methods**, "Measuring the frequency of lysogeny as a function of MOI and growth rate") as a function of the time when kanamycin was added after infection. MG1655 cells were infected by λ_{ts} at MOI ≈ 5 (using the same protocol described in **Supplementary Fig. 9**), and incubated at 30°C. At different times, 50 μg mL^{-1} kanamycin was added to the culture. Markers, data; error bars, SEM from technical replicates. Red line, average of the values at 30, 45, 60, and 90 minutes. When kanamycin was added immediately after infection (yellow highlight), the measured frequency was only 0.002.

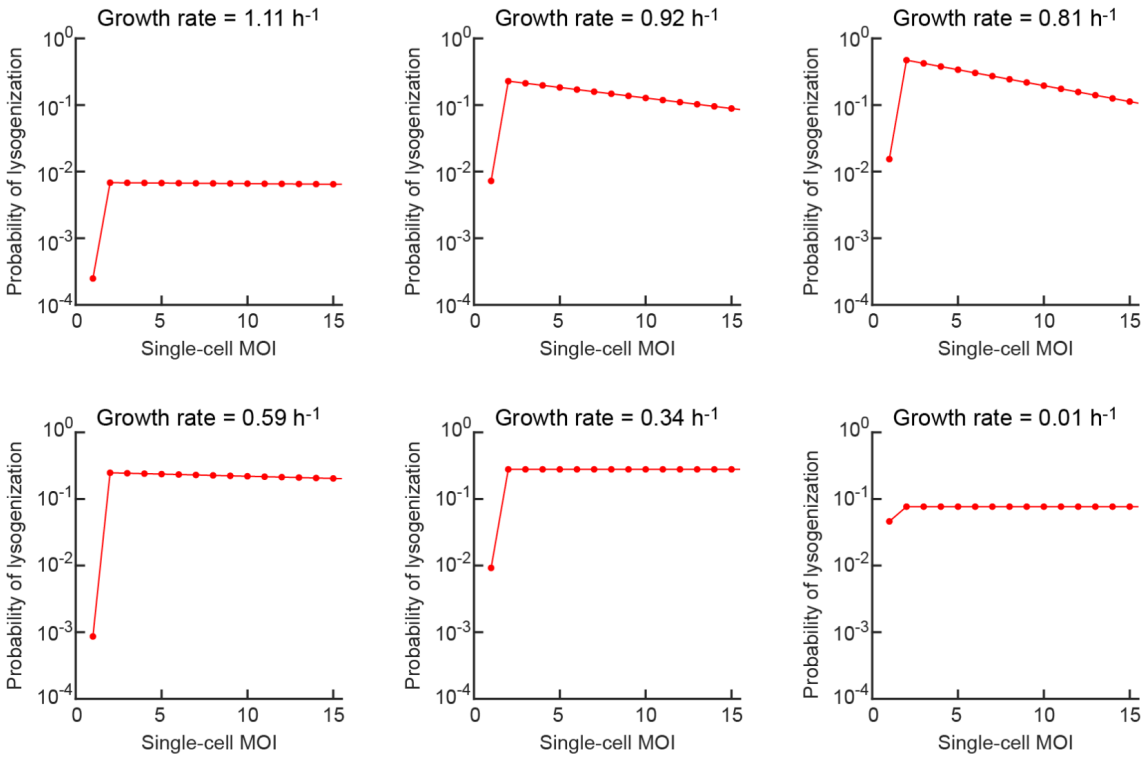

Supplementary Fig. 15: The inferred single-cell MOI response curve at different growth rates.

MG1655 cells at different growth rates were infected by λ_{ts} as described in **Methods**, "Measuring the frequency of lysogeny as a function of MOI and growth rate"**.** Markers, the probability of lysogenization (inferred using the product $Q_n R_n$, as described in **Methods**, "Inferring the single-cell probability of lysogenization") as a function of the single-cell MOI (n).

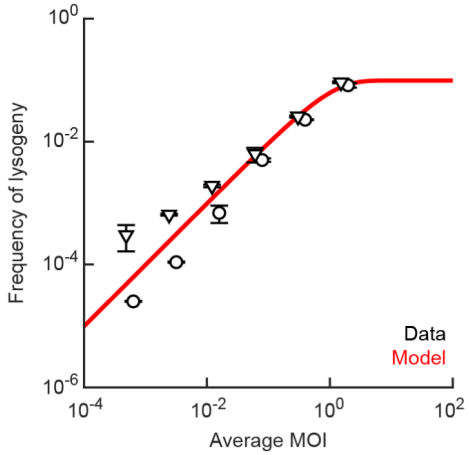

Supplementary Fig. 16: Fitting the frequency of lysogeny in stationary cells, using MOI* = 1.

MG1655 cells in stationary phase were infected by λ_{ts} as described in **Methods**, "Measuring the frequency of lysogeny as a function of MOI and growth rate"**.** Circles and triangles, data obtained in two independent runs of the experiment (reproduced from **Fig. 5b**); error bars, SEM. Red line, model fit using **Eq. (34)**, which assumes MOI* = 1 (in contrast to the model shown in **Fig. 5b**, fitted using **Eq. (33)**, which assumes MOI* = 2).

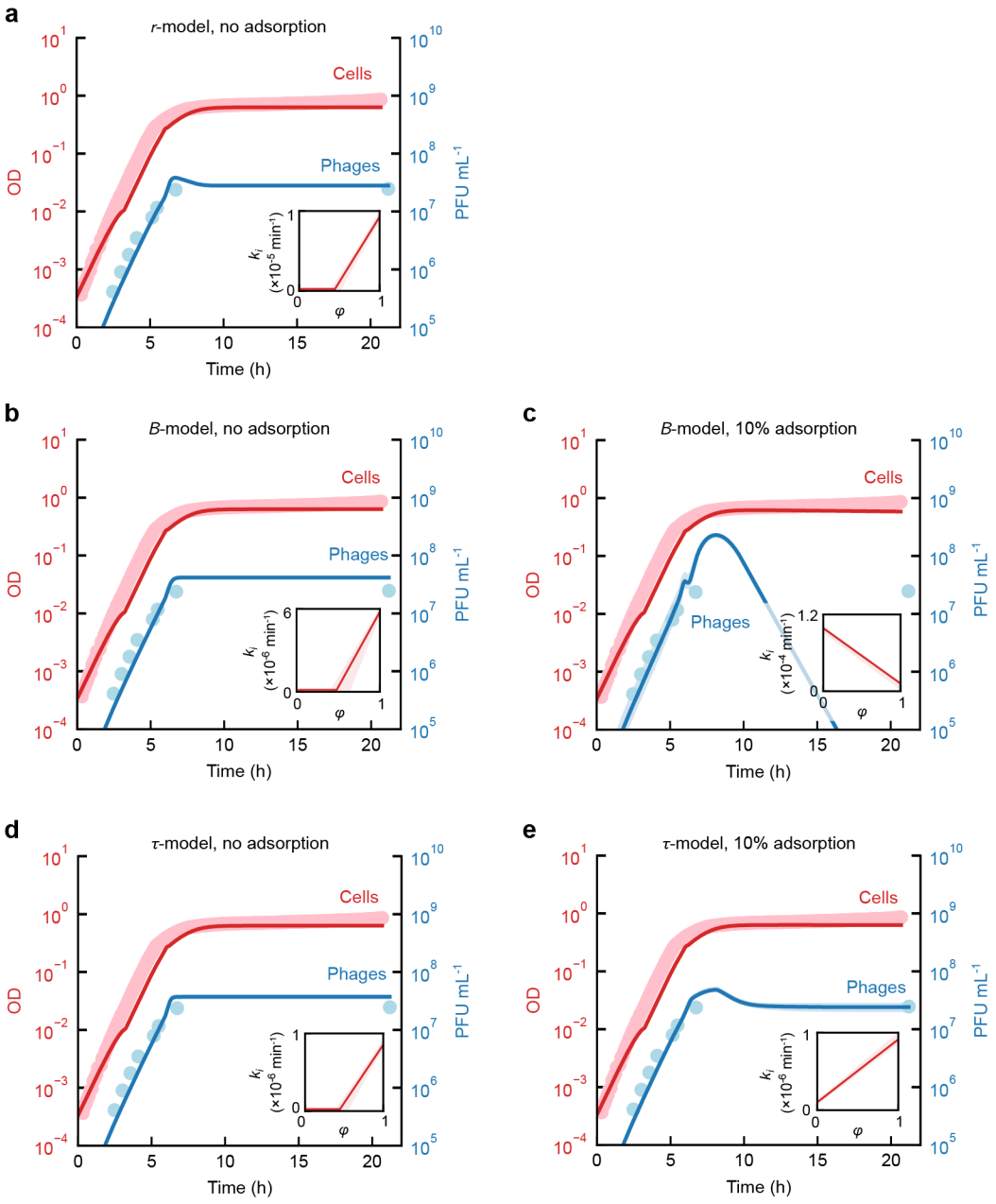

Supplementary Fig. 17: Modeling lysogen growth and phage dynamics using different assumptions.

Modeling OD (red) and phage concentration (blue) during growth of lysogens using different models. In each panel, markers, experimental data. Lines, model fitting. Shading, fits by the ensemble of parameters obtained using Markov chain Monte Carlo (MCMC). Inset, the inferred rate of spontaneous induction (k_i) as a function of the normalized instantaneous bacterial growth rate (φ). The fitting procedure is described in **Methods**, "Modeling spontaneous induction". The fitted parameters are shown in **Supplementary Table 5**. For the "r-model" with a 10% adsorption rate as in LBM, see **Fig. 5f**. The model assumptions for each panel are as follows: (**a**) "r-model", without adsorption; (**b**) "B-model", without adsorption; (**c**) "τ-model", without adsorption; (**d**) "B-model", with a 10% adsorption rate as in LBM; (**e**) "τ-model", with a 10% adsorption rate as in LBM.

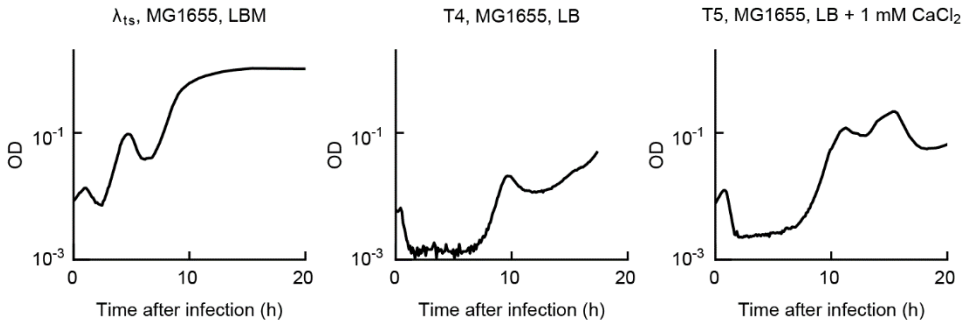

Supplementary Fig. 18: Multiple cycles of growth and lysis following phage infection.

Lines, growth curves of MG1655 cells when infected by phages λ_{ts}, T4, and T5 at MOI ≈ 1000. Infection mixtures were incubated at 37°C in LB medium (supplemented with 10 mM $MgSO_4$ for λ_{ts}, or 1 mM $CaCl_2$ for T5). The experimental protocol is described in **Methods**, "Microplate-based infection assay for measuring phage concentrations".

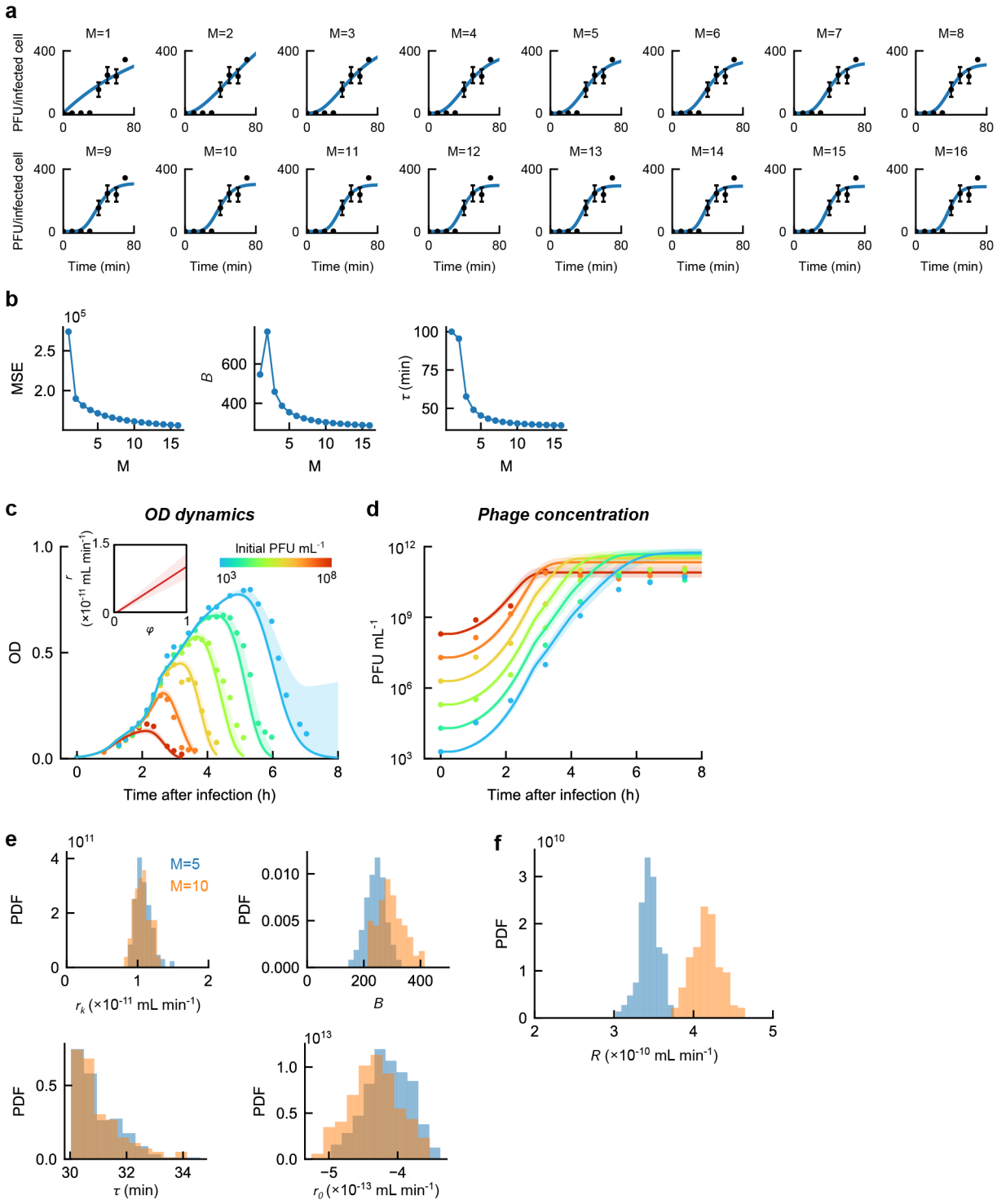
a
M=1
M=2
M=3
M=4
M=5
M=6
M=7
M=8
M=9
M=10
M=11
M=12
M=13
M=14
M=15
M=16
PFU/infected cell
Time (min)
b
MSE
B
τ (min)
M
c
OD dynamics
OD
Time after infection (h)
r (×10⁻¹¹ mL min⁻¹)
φ
Initial PFU mL⁻¹
10³
10⁸
d
Phage concentration
PFU mL⁻¹
Time after infection (h)
e
PDF
M=5
M=10
r_k (×10⁻¹¹ mL min⁻¹)
B
τ (min)
r_0 (×10⁻¹³ mL min⁻¹)
f
PDF
R (×10⁻¹⁰ mL min⁻¹)

Supplementary Fig. 19: Parameterizing the number of intermediate infection states (M).

(**a**) Model fitting for the phage dynamics from a one-step experiment (as shown in **Supplementary Fig. 9**), assuming different number of intermediate states (M). Markers, experimental data. Lines, model fits. The fitting procedure is described in **Methods**, "Parameterization of the number of intermediate infected states (M)". (**b**) The mean squared error (MSE) (right), fitted B (middle), and fitted τ (right) as a function of M. (**c**) Model fitting for the OD dynamics using "r-model", assuming M = 10. Colored markers, data from infection at different initial phage concentrations. Colored lines, best fit of the model. Colored shading, fits by the ensemble of parameters obtained using Markov chain Monte Carlo (MCMC). Inset, fitted r as a function of normalized instantaneous growth rate φ. (**d**) Prediction of the phage dynamics. Colored markers, data from infection at different initial phage concentrations. Colored lines, model predictions from the best-fit parameters. Shared regions, model predictions from the ensemble of parameters. The fitting and prediction procedures are described in **Methods**, "Examining model assumptions". (**e**) The distribution of parameter values when M = 5 (blue) or M = 10 (orange). (**f**) The distribution of the relative growth rate of viral population (R) in the two models.

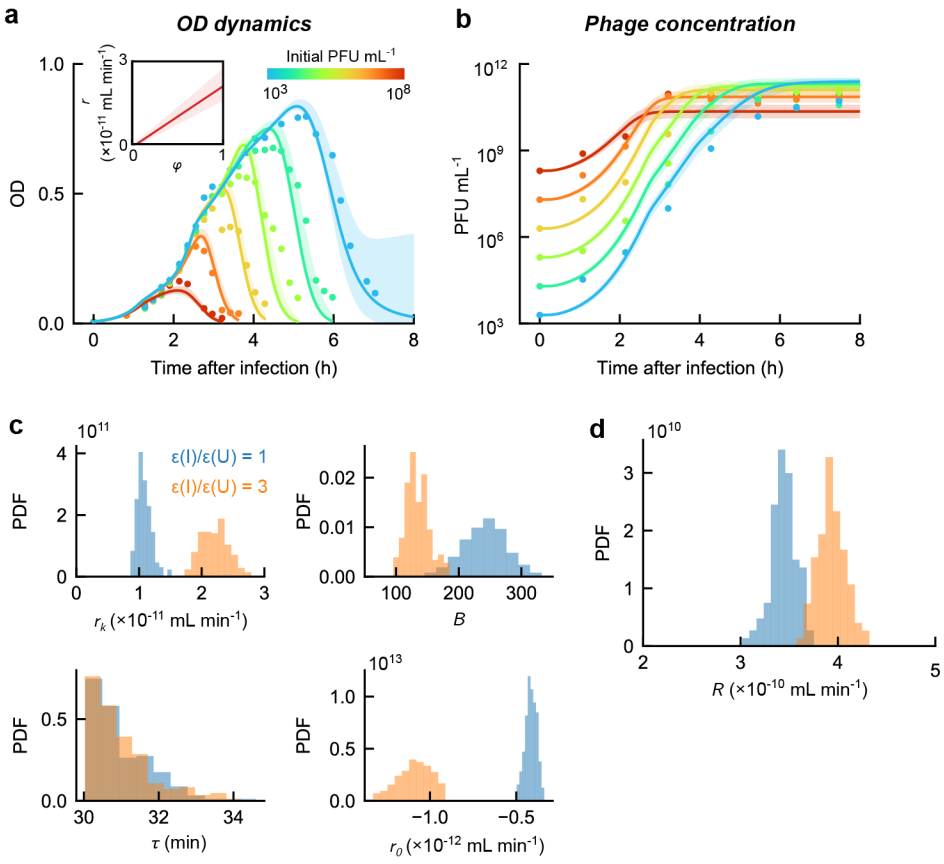

Supplementary Fig. 20: Modeling the increased length of infected cells.

(**a**) Model fitting for the OD dynamics using the "r-model", assuming the molar absorptivity (ε) of infected cells is three-fold of the uninfected cells. Colored markers, data from infection at different initial phage concentrations. Colored lines, best fit of the model. Colored shading, fits by the ensemble of parameters obtained using Markov chain Monte Carlo (MCMC). Inset, fitted r as a function of normalized instantaneous growth rate φ. (**b**) Prediction of the phage dynamics. Colored markers, data from infection at different initial phage concentrations. Colored lines, model predictions from the best-fit parameters. Shared regions, model predictions from the ensemble of parameters. The fitting and prediction procedures are described in **Methods,** "Examining model assumptions". (**c**) The distribution of parameter values, when the molar absorptivity of infected cells is the same as that of the uninfected cells (blue) or threefold of the uninfected cells (orange). (**d**) The distribution of the relative growth rate of viral population (R) in the two models.

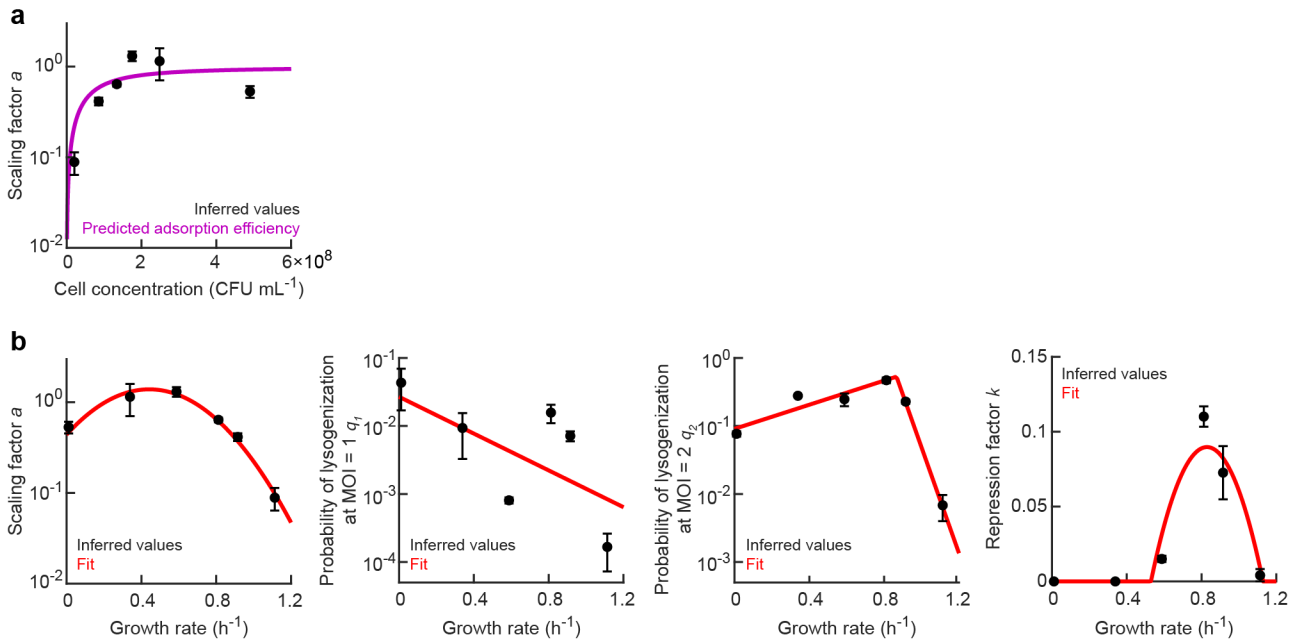

Supplementary Fig. 21: Parameterization of the frequency of lysogeny as a function of growth rate.

(**a**) The MOI-scaling factor a is consistent with the efficiency of phage adsorption. Markers, values of the parameter a, inferred as described in **Methods**, "Inferring the single-cell probability of lysogenization", following infection at different bacterial densities (**Methods**, "Measuring the frequency of lysogeny as a function of MOI and growth rate"); error bars, SEM from two independent runs of the experiment. Purple curve, prediction by the model in ref. [5] for maltose-containing medium at 30°C. (**b**) The parameters a, q_1, q_2, and k, inferred as described in **Methods**, "Inferring the single-cell probability of lysogenization", as a function of the bacterial growth rate upon infection. Markers, inferred values; error bars, SEM from two independent runs of the experiment (Values for a are reproduced from panel a). Red lines, parameterization using **Eq. (36)**. The parameter values are shown in **Supplementary Table 4**.

SUPPLEMENTARY TABLES

Supplementary Table 1: Bacterial and phage strains used in this study

Strain	Description	Source
BACTERIA		
MG1655	Wild-type *E. coli*	Lab stock
LE392	*glnV* (*supE*44), *tryT* (*supF*58); amber suppressor[6].	Lab stock
PHAGE		
λ_{ts}	λ *cI*857 *bor*::*kan*^{R} Temperature-sensitive; obligately lytic at 37ºC and above[7].	Lab stock
λ_{wt}	λ cI_{wt} *bor*::*kan*^{R} Wild-type.	Lab stock
T4		Coli Genetic Stock Center
T5		Coli Genetic Stock Center
P1*vir*	Virulent mutant	Lab stock

Supplementary Table 2: Fitted growth parameters under different growth conditions

Growth medium	Parameter	Description	Mean ± SEM
M9Mal	v_1	Maximum growth rate	0.019 ± 0.000 min^{-1}
	K_1	Affinity constant	1.0 ± 0.0
	e	Conversion efficacy parameter	2.1 ± 0.0
M9Glu	v_1	Maximum growth rate	0.022 ± 0.000 min^{-1}
	K_1	Affinity constant	1.0 ± 0.0
	e	Conversion efficacy parameter	2.1 ± 0.0
LBM	v_1	Maximum growth rate in phase 1	0.054 ± 0.002 min^{-1}
	v_2	Maximum growth rate in phase 2	0.019 ± 0.003 min^{-1}
	v_3	Maximum growth rate in phase 3	0.007 ± 0.001 min^{-1}
	K_1	Affinity constant for substrate in phase 1	0.68 ± 0.05
	K_2	Affinity constant for substrate in phase 2	0.74 ± 0.06
	K_3	Affinity constant for substrate in phase 3	0.42 ± 0.06
	θ_1	The nutrient concentration at which phase 1 ends	0.66 ± 0.02
	θ_2	The nutrient concentration at which phase 2 ends	0.40 ± 0.02
	e	Conversion efficacy parameter	0.43 ± 0.00
LBGM	v_1	Maximum growth rate in phase 1	0.031 ± 0.003 min^{-1}
	v_2	Maximum growth rate in phase 2	0.029 ± 0.003 min^{-1}
	v_3	Maximum growth rate in phase 3	0.014 ± 0.001 min^{-1}
	K_1	Affinity constant for substrate in phase 1	0.52 ± 0.13
	K_2	Affinity constant for substrate in phase 2	0.55 ± 0.09
	K_3	Affinity constant for substrate in phase 3	0.65 ± 0.04
	θ_1	The nutrient concentration at which phase 1 ends	0.72 ± 0.05
	θ_2	The nutrient concentration at which phase 2 ends	0.48 ± 0.05
	e	Conversion efficacy parameter	0.67 ± 0.00

Supplementary Table 3: Fitted infection parameters under different growth conditions

Growth medium	Model	Parameter	Range of prior	Best fit value	Range of ensemble of parameters
LBM	Null model	r	[10^{-12}, 10^{-10}] mL min^{-1}	3.1×10^{-11} mL min^{-1}	[2.4×10^{-11}, 4.1×10^{-11}] mL min^{-1}
		B	[10, 1000]	211.6	[140.5, 344.8]
		τ	[30, 150] min	64.5 min	[52.3, 81.2] min
	r-model: $r = \max(0, r_0 + r_k \cdot \phi)$	r_k	[10^{-12}, 10^{-10}] mL min^{-1}	1.42×10^{-11} mL min^{-1}	[8.5×10^{-12}, 2.4×10^{-11}] mL min^{-1}
		r_0	[10^{-12}, 10^{-10}] mL min^{-1}	-4.9×10^{-13} mL min^{-1}	[$-5e\times10^{-13}$, 2.8×10^{-12}] mL min^{-1}
		B	[10, 1000]	155.7	[96.5, 343.9]
		τ	[30, 150] min	30.0 min	[30.0, 35.3] min
	B-model: $B = \max(0, B_0 + B_k \cdot \phi)$	r	[10^{-12}, 10^{-10}] mL min^{-1}	1.24×10^{-11} mL min^{-1}	[9.4×10^{-12}, 1.5×10^{-11}] mL min^{-1}
		B_k	[10, 1000]	164.2	[143.5, 276.4]
		B_0	[-1000, 1000]	-4.9	[-11.3, -3.2]
		τ	[30, 150] min	30.0 min	[30.0, 34.1] min
	τ-model: $\tau = \max(20, \tau_0 + \tau_k \cdot \phi)$	r	[10^{-12}, 10^{-10}] mL min^{-1}	8.1×10^{-12} mL min^{-1}	[4.3×10^{-12}, 1.2×10^{-11}] mL min^{-1}
		B	[10, 1000]	150.9	[84.6, 370.4]
		τ_k	[-1000, 1000] min	-357.9 min	[-438.7, -298.3] min
		τ_0	[0, 1000] min	119.4 min	[101.8, 142.7] min
M9Mal	Null model	r	[10^{-11}, 10^{-8}] mL min^{-1}	6.3×10^{-10} mL min^{-1}	[5.2×10^{-10}, 7.9×10^{-10}] mL min^{-1}
		B	[10, 1000]	150.0	[97.8, 213.4]
		τ	[30, 150] min	51.8 min	[46.9, 59.1] min
M9Glu	Null model	r	[10^{-11}, 10^{-8}] mL min^{-1}	7.5×10^{-11} mL min^{-1}	[7.0×10^{-11}, 7.8×10^{-11}] mL min^{-1}
		B	[10, 1000]	563.4	[515.9, 661.7]
		τ	[30, 150] min	106.0 min	[103.7, 109.1] min

Supplementary Table 4: Fitted frequency of lysogeny as a function of MOI and growth rate

Parameter	Mean ± SEM
$\boldsymbol{a}$	
β_2	-5.89 ± 0.87
β_1	5.21 ± 1.02
β_0	-0.82 ± 0.31
$\boldsymbol{q_1}$	
β_1	-3.11 ± 1.33
β_0	-3.62 ± 0.85
$\boldsymbol{q_2}$	
β_1	2.04 ± 0.00
β_0	-2.04 ± 0.00
β_2	17.89 ± 0.00
g^*	0.87 ± 0.00
$\boldsymbol{k}$	
g_1	0.53 ± 0.06
g_2	1.13 ± 0.06

Supplementary Table 5: Fitted induction rates using different models

Model	Parameter	Range of prior	Best fit value	Range of ensemble of parameters
r-model + no adsorption	k_{i_k}	$[10^{-7}, 10^{-4}]$ min^{-1}	1.6×10^{-5} min^{-1}	$[1.5\times10^{-5}, 1.8\times10^{-5}]$ min^{-1}
	k_{i_b}	$[-10^{-4}, 10^{-4}]$ min^{-1}	-7.0×10^{-6} min^{-1}	$[-9.0\times10^{-6}, -6.2\times10^{-6}]$ min^{-1}
B-model + no adsorption	k_{i_k}	$[10^{-7}, 10^{-4}]$ min^{-1}	1.1×10^{-5} min^{-1}	$[1.0\times10^{-5}, 1.5\times10^{-5}]$ min^{-1}
	k_{i_b}	$[-10^{-4}, 10^{-4}]$ min^{-1}	-5.1×10^{-6} min^{-1}	$[-9.3\times10^{-6}, -4.1\times10^{-6}]$ min^{-1}
τ-model + no adsorption	k_{i_k}	$[10^{-7}, 10^{-4}]$ min^{-1}	1.5×10^{-6} min^{-1}	$[1.4\times10^{-6}, 1.8\times10^{-6}]$ min^{-1}
	k_{i_b}	$[-10^{-4}, 10^{-4}]$ min^{-1}	-6.4×10^{-7} min^{-1}	$[-9.4\times10^{-7}, -5.6\times10^{-7}]$ min^{-1}
r-model + 10% adsorption	k_{i_k}	$[10^{-7}, 10^{-4}]$ min^{-1}	2.1×10^{-5} min^{-1}	$[1.9\times10^{-5}, 2.7\times10^{-5}]$ min^{-1}
	k_{i_b}	$[-2\times10^{-5}, 2\times10^{-5}]$ min^{-1}	-1.0×10^{-5} min^{-1}	$[-1.5\times10^{-5}, -7.5\times10^{-6}]$ min^{-1}
B-model + 10% adsorption	k_{i_k}	$[10^{-7}, 10^{-4}]$ min^{-1}	-8.6×10^{-5} min^{-1}	$[-9.5\times10^{-5}, -8.6\times10^{-5}]$ min^{-1}
	k_{i_b}	$[-10^{-4}, 10^{-4}]$ min^{-1}	9.9×10^{-5} min^{-1}	$[9.4\times10^{-5}, 10.0\times10^{-5}]$ min^{-1}
τ-model + 10% adsorption	k_{i_k}	$[10^{-7}, 10^{-4}]$ min^{-1}	8.1×10^{-7} min^{-1}	$[7.7\times10^{-7}, 8.8\times10^{-7}]$ min^{-1}
	k_{i_b}	$[-10^{-4}, 10^{-4}]$ min^{-1}	1.0×10^{-7} min^{-1}	$[8.8\times10^{-8}, 1.2\times10^{-7}]$ min^{-1}

SUPPLEMENTARY REFERENCES

1. Sezonov, G., Joseleau-Petit, D. & D'Ari, R. *Escherichia coli* Physiology in Luria-Bertani Broth. *J Bacteriol* **189**, 8746–8749 (2007).
2. Yao, T., Coleman, S., Nguyen, T. V. P., Golding, I. & Igoshin, O. A. Bacteriophage self-counting in the presence of viral replication. *Proc. Natl. Acad. Sci. U.S.A.* **118**, e2104163118 (2021).
3. Nabergoj, D., Modic, P. & Podgornik, A. Effect of bacterial growth rate on bacteriophage population growth rate. *MicrobiologyOpen* **7**, e00558 (2018).
4. Hadas, H., Einav, M., Fishov, I. & Zaritsky, A. Bacteriophage T4 Development Depends on the Physiology of its Host Escherichia Coli. *Microbiology* **143**, 179–185 (1997).
5. Moldovan, R., Chapman-McQuiston, E. & Wu, X. L. On Kinetics of Phage Adsorption. *Biophysical Journal* **93**, 303–315 (2007).
6. Hendrix, R. W. *Lambda II*. (Cold Spring Harbor Laboratory, Cold Spring Harbor, N.Y, 1983).
7. Zong, C., So, L., Sepúlveda, L. A., Skinner, S. O. & Golding, I. Lysogen stability is determined by the frequency of activity bursts from the fate-determining gene. *Mol Syst Biol* **6**, 440 (2010).